KTH Electrical Engineering

MEMS tunable polarization rotator for optical communication

Sandipan Das

Stockholm, February 11, 2016

Contents

Chapter 1
1 Introduction

1.1 Light for communication using optical fibers

Communication and collective thinking are the key to the development of human civilization. This development is driven by data - "The new oil of this digital era". With the advent of Internet of Things (IoT), it has been estimated that by 2020 there will be 26 billion connected devices [1], and all devices that can be connected will be connected. Today, only about 40% [2] of the world's population use the internet and the amount of data produced per minute in the internet through different channels is already growing exponentially.

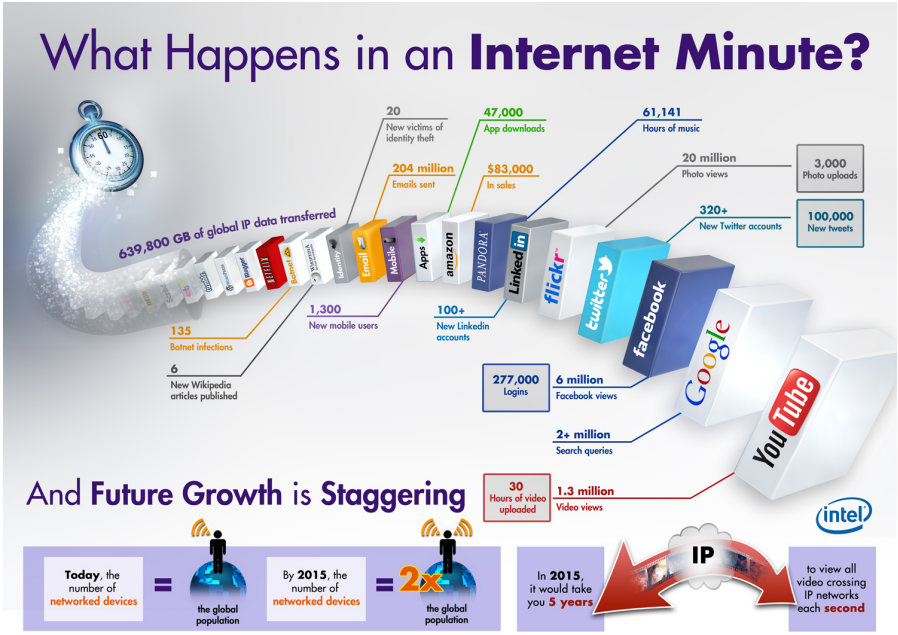

Figure 1.1: What happens on internet per minute [3]

Eventually, as more and more people use the different Information and communication technology (ICT) services, this data growth will be higher than ever.

Also, with the advent of smart-phones, there has been a huge surge in data traffic all over the world. It has been estimated in Ericsson's mobility report [4] that 70% of

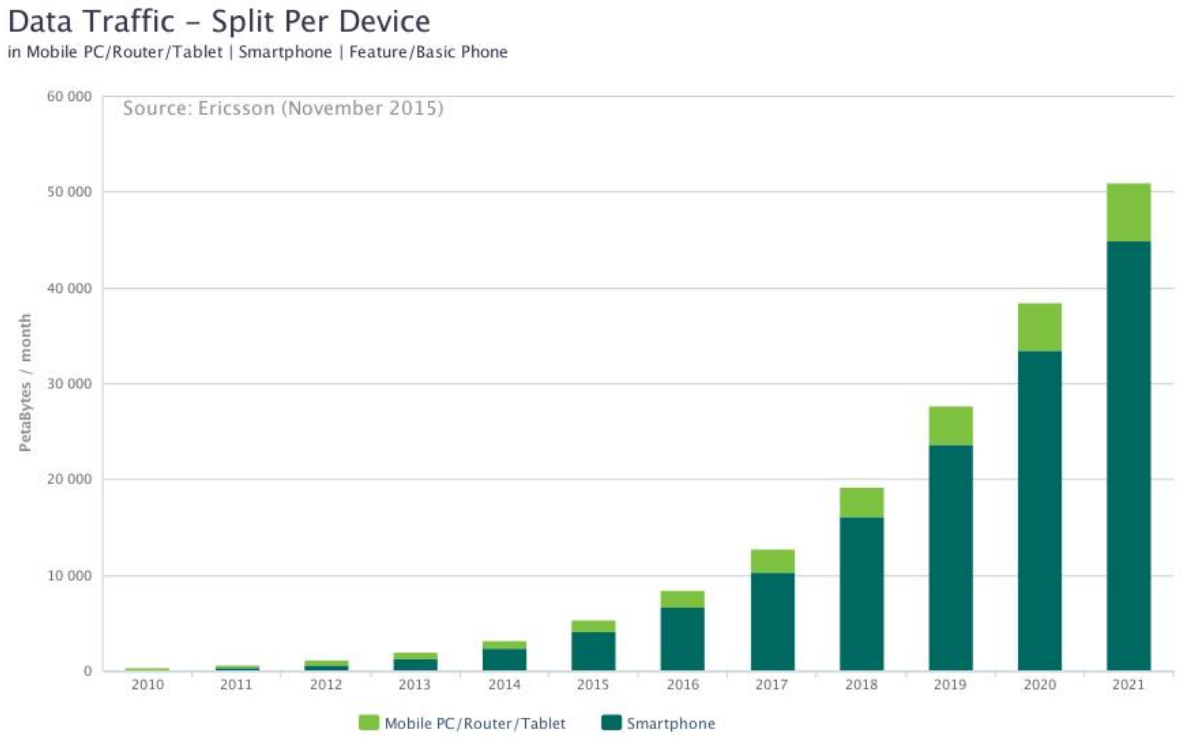

Figure 1.2: Data traffic growth forecast by 2020, as per Ericsson, generated using [5] [3]

world's population will use smart-phones by 2020 and 90% of the world's population over 6 years old will have a mobile phone by 2020.

Currently, the telecommunications industry is moving towards IP Multimedia Subsystem (IMS) core networks which is a transition towards full IP based networks. So how is this traffic managed? The answer is the optical fiber, which serves as the backbone of all the communication systems. Optical fiber is chosen over previously used copper cables for the following reasons:

- ☐ Fiber provides more bandwidth than copper and has standardized performance up to 100 Gbps and beyond, at very low power.
- ☐ Fiber is also less susceptible to temperature fluctuations than copper and can be submerged in water for intercontinental long distance communication. It's immune to Electromagnetic (EM) interference and radio-frequency Radio frequency (RF) interference, crosstalk, impedance problems etc.
- ☐ It doesn't radiate signals and is extremely difficult to tap, which provides better security than copper cables.
- ☐ Fiber optic transmission results in less attenuation than copper cables.

1.2 Silicon photonics for optical communication

The performance of optical fiber network is remarkable and it is this backbone which gives us an unfathomable user experience. The current internet architecture has already pushed the optical fiber to the network edges and the trend is to push it as closer to the processor as possible. This has already opened up a new trend of "siliconizing photonics" [7] based on the decades of research from microelectronics industry. The electronics industry has pushed the boundaries of the processing speed of Integrated circuit(s) (IC) according to Moore's Law, after the discovery of semiconductors. Until recently, exponential increases in the speed, efficiency, and processing power of conventional electronic devices were achieved largely through the downscaling and clustering of components on a chip. However, this trend toward miniaturization has yielded unwanted effects in the form of significant increases in noise, power consumption, signal propagation delay and aggravates already to serious thermal management problems. Alternatively, the wires can be made thicker, but then the packing density will be inefficient. As a result, traditional microelectronics will soon fall short of meeting market needs, inhibited by the thermal and bandwidth bottlenecks inherent in copper wiring. Intel processor speed and bus speed comparison [6] shows that although we have achieved good processing speed, the interconnects always find difficulty in catching up with the processing speed. Think of a data center processing tera-bytes of data per minute, where interconnects between processors can add up to a significant bottleneck. These bottlenecks can be overcome by substituting copper with optical interconnects using the current technology, which can also operate at low power and better efficiency. In addition optical interconnects can also reduce power consumption caused by heat dissipation, switching and transmission of electrical signals.

have to make sure

Although silicon is the optimal material for electronics, only recently silicon is being considered as a practical option for Optoelectronic integrated circuit (OEIC) solutions. Silicon has many properties conducive to fiber optics. The band gap of silicon ($\sim$1.1 eV) is such that the material is transparent to wavelengths commonly used for optical transport ($\sim$1.3 µm-1.6 µm). One can use standard Complementary metal-oxide semiconductor (CMOS) processing techniques to sculpt optical waveguides onto the silicon surface. Similar to an optical fiber, these waveguides can be used to confine and direct light as it passes through the silicon [34] using total internal reflection. Due to the wavelengths typically used for optical transport and silicon's high index of refraction, the feature sizes needed for processing these silicon waveguides are on the order of 0.5 µm-1 µm. The fabrication and lithography requirements needed to process waveguides with these sizes exist today. Finally, if all this remains CMOS-compatible, it could be possible to process monolithic optical devices, which could bring new levels of performance, functionality, power and size reduction, all at a lower cost.

Today silicon photonics technology is a new approach to make optical devices out of silicon and use light (photons) to move huge amounts of data at very high speeds with extremely low power over a thin optical fiber rather than using electrical signals over a copper wire. Since, already enough capital investments has been done on perfecting the current fabrication technology and infrastructure, engineers are working on creating

monolithic design of integrated circuits which will use light in place of electric signals [8]. Research institutes in collaboration with industry partners, are trying to bridge this gap by creating highly integrated photonic and electronic components that combine the functionality of conventional CMOS circuits with the significantly enhanced system performance of photonic solutions. Various kinds of silicon photonic devices such as, switches [12, 13, 14], modulators [15, 16], photodetectors [17, 18], delay lines [19, 20], sensors [21, 22, 23] etc. have been reported till date. It is also promising in developing on-chip integration for telecommunications applications and servers in data centers [11]. The silicon photonics market is estimated to grow to 700 million USD by 2024 [10] with a Compound annual growth rate (CAGR) of 38%.

Previously, you had marked it when i wrote organization here

1.3 Motivation

All photonic devices based on silicon waveguides are sensitive to polarization due to large structural birefringence, which induces substantial Polarization dependent loss (PDL), Polarization mode dispersion (PMD), and Polarization dependent wavelength characteristics (PDλ), limiting their usability. To overcome these challenges, Polarization rotator (PR)s are engineered on silicon for OEIC and various designs have already been demonstrated [24, 25, 26, 27, 28, 29, 30]. The main working principle of these proposed solutions is introducing asymmetry in the waveguide structure which changes the effective Refractive index (RI). Also, in some cases the designs [31], if used in commercial applications for miniature interconnects, would incur inefficient packing density since too much space is required to achieve high and robust tuning. Apart from that there might also be thermo-optic induction problem which might change phase of the wave in other waveguides in high compact density environment as silicon is highly susceptible to thermal changes [32]. Also, a Tunable polarization rotator (TPR) has been reported which works on the principle of Berry's phase, a quantum-mechanical phenomenon of purely topological origin [33]. For PR, the design uses out-of-plane ring cavity which inherits the narrow band spectral features of ring resonator limiting the bandwidth. Phase tuning is achieved through thermo-optic effect which has its limitations. The general goal of the thesis work is to realize an efficient TPR using Microelectromechanical systems (MEMS), at low power with high precision and accuracy.

1.4 Objectives

Main objective: To design and fabricate low power TPR based on MEMS tuning.

Sub objectives: The areas which will be addressed are:

- ☐ Feasibility of the idea and the strategy to design the PR.
- ☐ Design and simulation of the device.
- ☐ Fabrication and characterization of the MEMS tunable PR.

1.5 Outline of this thesis

The outline of the thesis is as follows: Background, motivation and the research questions being addressed, is discussed in Chapter 1. In Chapter 2, the current state of art for the available solution is discussed along with the background literature required. Here, also the working principle of the current available design are explained along with the areas which can be improved. Chapter 3 discusses about the design of the final system and the results obtained about the simulation setup. In Chapter 4, documentation about the fabricated design is provided along with currently available standard fabrication technologies. Results and characterization are an important part of the work, which is discussed in Chapter 5. Finally, Chapter 6 and 7 discusses about the conclusion and future work possibilities respectively along with the known limitations of the system if any.

Chapter 2
2 State of the art

To understand the available PR it is important to look into the basic concepts of waveguides and the mathematics behind the propagation of EM waves in waveguides. It is also necessary to understand tuning of optical waveguides using different mechanisms to achieve optical polarization. Finally, the currently available PRs and their underlying concepts are discussed.

2.1 Optical waveguide theory

Light can travel through dielectric waveguide. To comprehend the situation we need to look at physical properties of light and waveguides. The basic understanding of Maxwell's equations are required, which combine the electric and magnetic fields to and produce a wave equation. Since, the optical system changes polarization we need a formal definition of the different State of polarization (SOP), described using Jones calculus. Moreover, the transition from one SOP to another, can be defined formally on the Poincaré sphere.

2.1.1 Maxwell's equations

EM radiation is the radiant energy released by varying EM field. Light wave is EM radiation at very high frequency. The frequency of visible light falls in between IR and UV EM wave. James Clerk Maxwell discovered that he could combine four simple equations, which had been previously discovered, along with a slight modification to describe self-propagating waves of oscillating electric and magnetic fields [35]. The understanding of propagating of light waves using Maxwell's equations in a dielectric medium, is the key to the construction of waveguides. Maxwell's equations relate the electric field E (V/m), magnetic field H (A/m), charge density ρ (C/m3), and current density J (A/cm2).

- **Maxwell's first equation (Gauss' Law)**: The net electric flux through any closed surface is equal to $\frac{1}{\epsilon_m}$ times the charge density within that closed surface.

$$\nabla.E = \frac{\rho}{\epsilon_m} \tag{2.1}$$

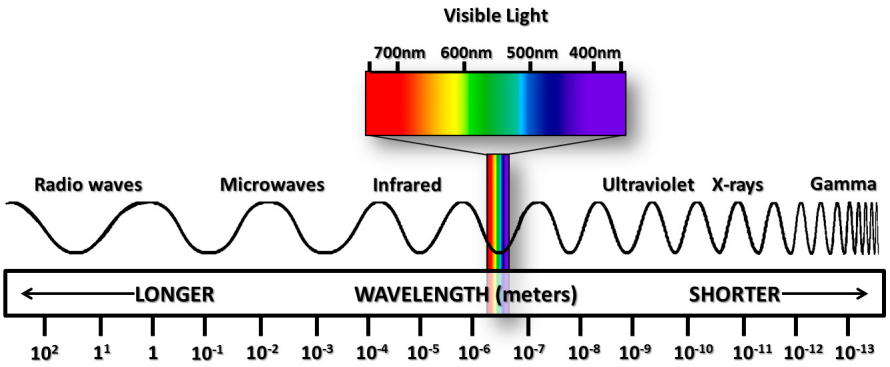

Figure 2.1: The EM wave spectrum

where ϵ_m the permittivity of the medium, and del operator, ∇, is given by:

$$\nabla = \left(\frac{\partial i}{\partial x}, \frac{\partial j}{\partial y}, \frac{\partial k}{\partial z}\right) \tag{2.2}$$

where i, j and k are unit vectors in the x, y and z directions respectively.

- **Maxwell's second equation (Gauss' Law for magnetic field)**: The net magnetic flux through a closed surface is always zero since magnetic monopoles do not exist.

$$\nabla.H = 0 \tag{2.3}$$

- **Maxwell's third equation (Faraday's law)**: Induced electric field around a closed path is equal to the negative of the time rate of change of magnetic flux enclosed by the path.

$$\nabla \times E = -\mu_m \frac{\partial H}{\partial t} \tag{2.4}$$

where μ_m is the magnetic permeability of the medium.

- **Maxwell's fourth equation (Modification of Ampere's law)**: The fourth equation states that magnetic fields can be generated in two ways: by electric current (this was the original "Ampere's law") and by changing electric fields (this was "Maxwell's addition") [36].

$$\nabla \times H = J + \epsilon_m \frac{\partial E}{\partial t} \tag{2.5}$$

These equations combine into the wave equation after some mathematical calculations.

$$\nabla^2 E - \mu_m \epsilon_m \frac{\partial^2 E}{\partial t^2} = \mu_m \frac{\partial J}{\partial t} + \frac{\nabla \rho}{\epsilon_m} \tag{2.6}$$

using the curl of curl identity operation given by:

$$\nabla^2 E = \nabla(\nabla.E) - \nabla \times (\nabla \times E) \tag{2.7}$$

A general solution to the equation 2.6 in free space, in absence of charge gives the following solution:

$$\overrightarrow{E}(z,t) = E_0(x,y)e^{i(k_0 z \pm \omega t)} \tag{2.8}$$

where z is direction of propagation of wave in Cartesian coordinates, phase, $\phi = k_0 z \pm \omega t$ and wave vector propagation constant, $k_0 = \dfrac{\partial \phi}{\partial t} = \dfrac{2\pi}{\lambda}$, in the direction of propagation of the wave. Propagation constant in medium varies according to n, the effective RI of the medium and is given by:

$$k = nk_0 \tag{2.9}$$

where,

$$n = \sqrt{\varepsilon_m \mu_m} \tag{2.10}$$

Similar calculations for the magnetic field, H in free space yields,

$$\overrightarrow{H}(z,t) = H_0(x,y)e^{i(k_0 z \pm \omega t)} \tag{2.11}$$

In the Fig. 2.2 the electric field and magnetic field propagate in directions perpendicular to each other. Moreover, the direction of propagation is also transverse to the EM field. Hence it is called Tansverse Electromagnetic (TEM) wave.

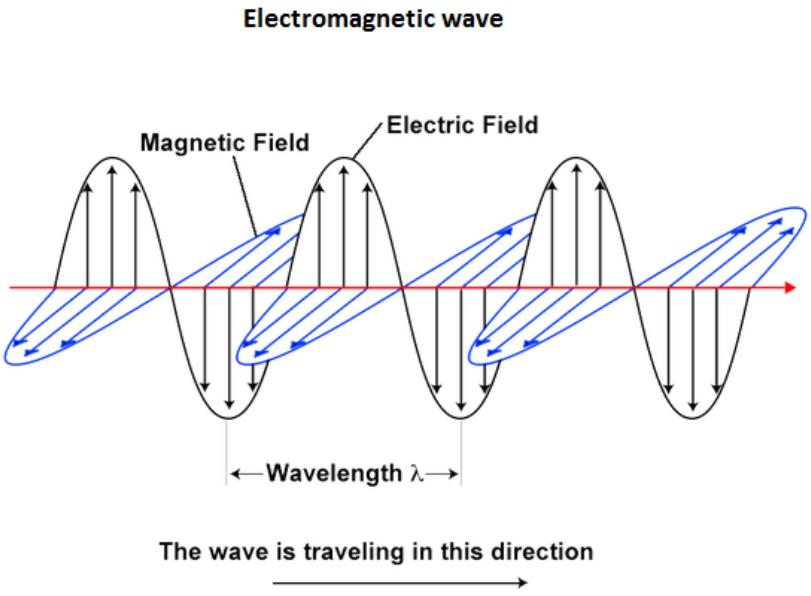

Figure 2.2: Propagation of EM wave

2.1.2 Optical waveguides

Waveguide is the essential element of every photonic circuit which can be characterized by the number of dimensions in which light is confined inside it [37]. A planar waveguide confines light in 1-D, which is simple for understanding of the wave propagation using Maxwell's equations. However, for practical applications 2-D confinement is necessary and that is why channel waveguides are used. Structures like photonic crystals even have 3-D confinement properties.

2.1.2.1 Planar waveguides

A simple planar waveguide consists of a high-indexed medium with height h surrounded by lower indexed materials on the top and bottom sides. The RI of the film, n_f (generally made from Si) is greater than the RI of the materials on the other sides. The RI of the substrate in lower cladding is n_s, (generally made from SiO_2) whereas, RI of the substrate in upper cladding is n_c (generally which is air).

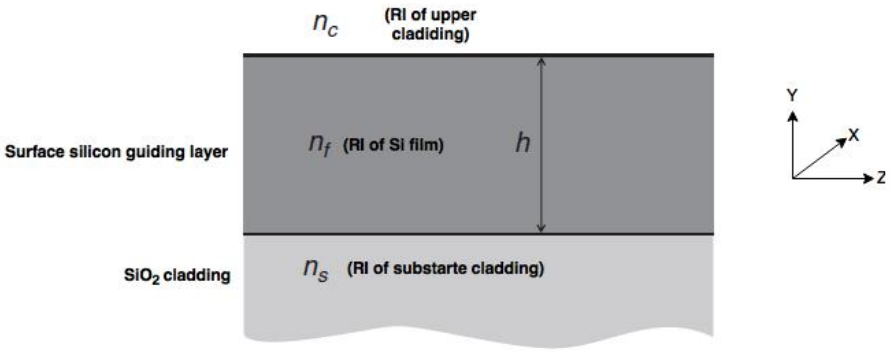

Figure 2.3: A typical planar waveguide where the film is infinite in XZ-plane

For planar waveguides the wave equation for electric field 2.8 and magnetic field can be rewritten as 2.11 follows:

$$\begin{cases} \overrightarrow{E}(z,t) = E_x(y)e^{i(k_0 z \pm \omega t)} \\ \overrightarrow{H}(z,t) = H_x(y)e^{i(k_0 z \pm \omega t)} \end{cases} \tag{2.12}$$

since in X-direction the film is infinite. After using the homogeneous wave equations for a planar waveguide the following Tansverse Electric (TE) and Tansverse Magnetic (TM) mode equations can be deduced:

$$\begin{cases} \nabla^2 E_x(y) + (k_0^2 n(y)^2 - k^2)E_x(y) = 0 \\ \nabla^2 H_x(y) + (k_0^2 n(y)^2 - k^2)H_x(y) = 0 \end{cases} \tag{2.13}$$

where RI depends only on a single Cartesian coordinate $n = n(y)$. These equations can be solved using the various boundary conditions of the waveguides which help in

deducing the nature of propagation of the wave in TE and TM mode. Different kinds of numerical methods like Finite element modeling (FEM), Finite difference time domain (FDTD), Beam propagation method (BPM) have been developed to decipher the nature of light propagation in waveguides.

2.1.2.2 Channel waveguides

As mentioned earlier channel waveguides provide confinement in 2-D which helps in depicting more practical waveguides. The three main types of channel waveguides are rib, strip and buried waveguides. As depicted in 2.4a, 2.4b, 2.4c the different conceptual structures of the waveguides can be envisaged. While the rib and strip waveguides are designed using etching technique, the buried waveguide mostly relies on diffusion and epitaxial growth technique for its fabrication.

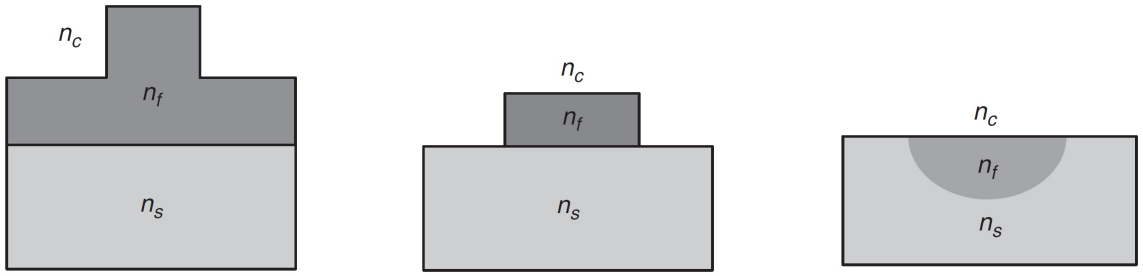

(a) Rib waveguide (b) Strip waveguide (c) Buried waveguide

Figure 2.4: Different kinds of design for channel waveguides

- **Design rules of rib waveguides:** While designing these waveguides each of these have specific design rules for optimum performance and low-loss coupling, which has been standardized after years of research [37]. The Single-mode condition (SMC) for *rib waveguides* is as follows:

$$\frac{W}{H} \leq 0.3 + \frac{r}{\sqrt{1-r^2}}, \quad \text{for } (0.5 \leq r < 1) \tag{2.14}$$

where W=waveguide width, H=rib height, r is ratio of slab height to overall rib height.

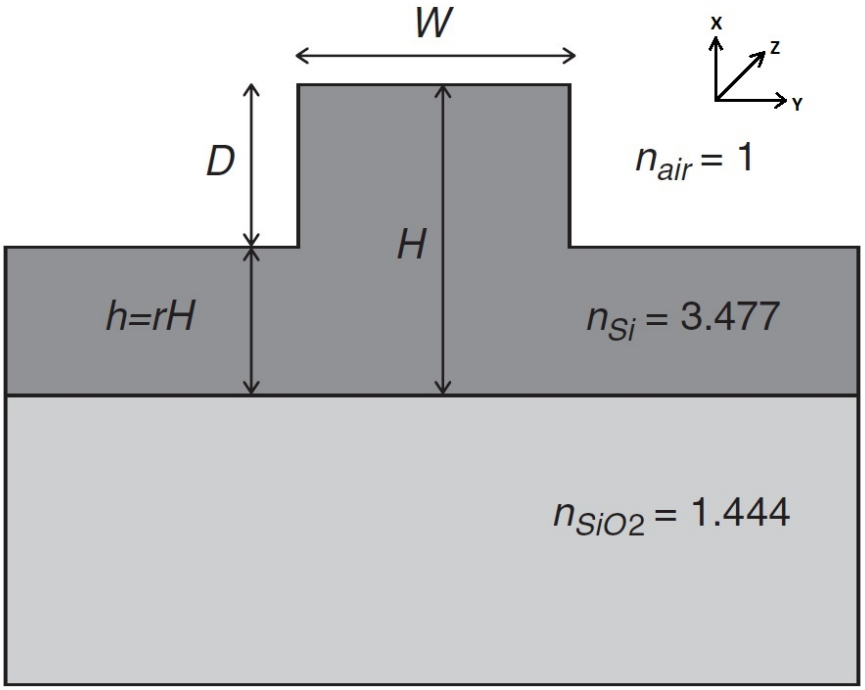

Figure 2.5: Rib waveguide design rules

The main requirements of the waveguide to cater the propagation of waves is that the dimension of the waveguide has to be more than the wavelength of the propagating wave. However, depending on the required structure the design rules may change which can be found using simulation.

- **Design rules of strip waveguides:** In mode confinement of light in optical waveguides the effective mode RI is important. Strip waveguides offer more high RI contrast in comparison to Rib waveguides. This can help in realization of ultra-dense photonic circuits because of high effective mode confinement. This can also achieve small bends which can improve the characterization of different monolithic optical circuits. In general a mix of rib and strip waveguides are used to achieve the desired circuitry, since sometimes the side walls cannot be etched in a perfectly smooth way causing greater evanescent fields from the waveguides introducing unnecessary coupling and losses. Using simulation for the desired scenario the robust values of the dimensions can be achieved.

2.1.3 Snell's law and total internal reflection

2.1.4 Eigenvalue and wave modes

In general, the electric field in the wave equation in 2.8 can be written in its constituent parts in Cartesian coordinates as:

$$\overrightarrow{E} = E_x i + E_y j + E_j k \tag{2.15}$$

If the wave propagates towards z-direction through any waveguide medium and is a TEM wave front then we will have a constant electric field vector in the z-direction. In this case there will be different solutions for the propagation constant, k in x and y directions. Now for each solution we can also get certain discrete angles at which the electric field can travel through the medium, which infers that light can propagate only at certain discrete angles through any dielectric medium. Each allowed solution is referred to as the *mode of propagation* and are basically the different eigenvalues of the propagation vector.

The eigenvalues provide the different acceptance angles at which light can be inserted into the waveguide, resulting in different modes in the waveguide. Depending on the dimensions of the waveguide, various modes can be found which are the different eigenvalues of the wave solution 2.8 and 2.11. For example, when light travels through optical fibers different modes can be visualized as follows in Fig. 2.6.

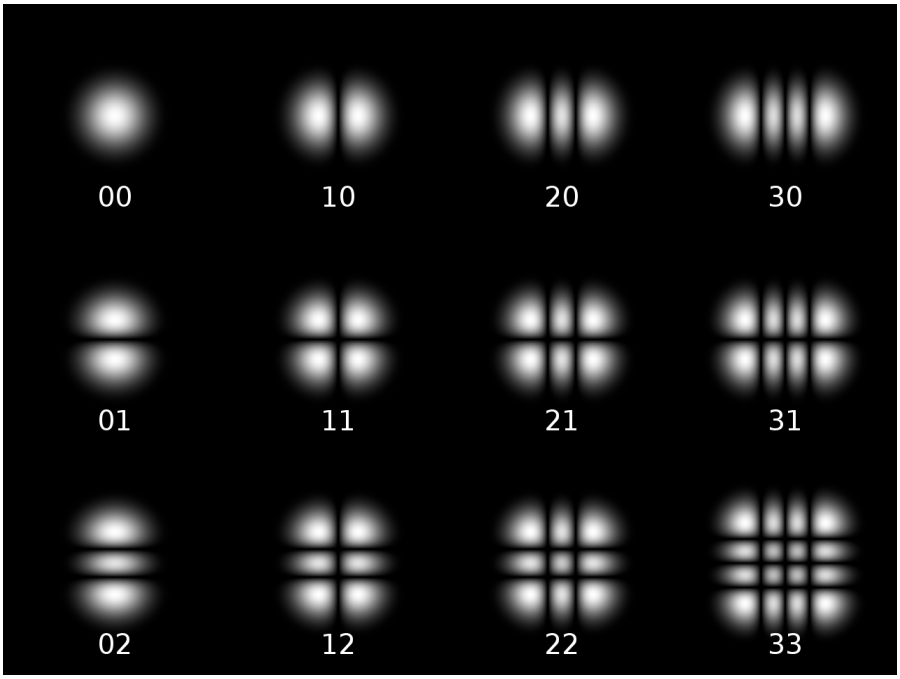

Figure 2.6: Rectangular transverse mode patterns TE(mn)

May be update the picture using CST simulation

2.1.5 Optical polarization and transverse modes

In optical waveguide, the transmission distance is limited by several types of dispersion, or spreading of optical pulses as they travel along the waveguide. Dispersion in waveguide is caused by a variety of factors. Intermodal dispersion, caused by the different axial speeds of different transverse modes, limits the performance of multi-mode waveguide. Because single-mode waveguide supports only one transverse mode, intermodal dispersion is eliminated. In single-mode performance is primarily limited by chromatic dispersion (also called group velocity dispersion), which occurs because the RI of silicon varies

slightly depending on the wavelength of the light, and light from real optical transmitters necessarily has nonzero spectral width (due to modulation). PMD, another source of limitation, occurs because although the single-mode waveguide can sustain only one transverse mode, it can carry this mode with two different polarizations, and slight imperfections or distortions in a waveguide can alter the propagation velocities for the two polarizations. This phenomenon is called birefringence and can be counteracted by polarization-rotator. PMD limits the bandwidth of the waveguide because the spreading optical pulse limits the rate that pulses can follow one another on the waveguide and still be distinguishable at the receiver.

Polarization is the direction of the electric field associated with the propagating wave. In the example in Fig. 2.2 the wave is polarized since the electric field and magnetic field exist in one direction only. In a dielectric optical waveguide, light propagates in plane polarized modes and the plane in which light is polarized is either vertical or horizontal to the direction of wave, as shown in Fig. 2.7 in single-mode.

2.1.5.1 TE mode

TE mode is the fundamental mode in which there is no electric field in the direction of propagation of light. In Fig. 2.7 the electric field lines (blue) are perpendicular to the plane of incidence in TE mode. The plane of incidence is the plane in which optical waves strike the surface of the waveguide.

2.1.5.2 TM mode

TM mode is the fundamental mode in which there is no magnetic field int he direction of propagation of light. In Fig. 2.7 it can be seen that magnetic field (red lines) are perpendicular to the plane of incidence in TM mode.

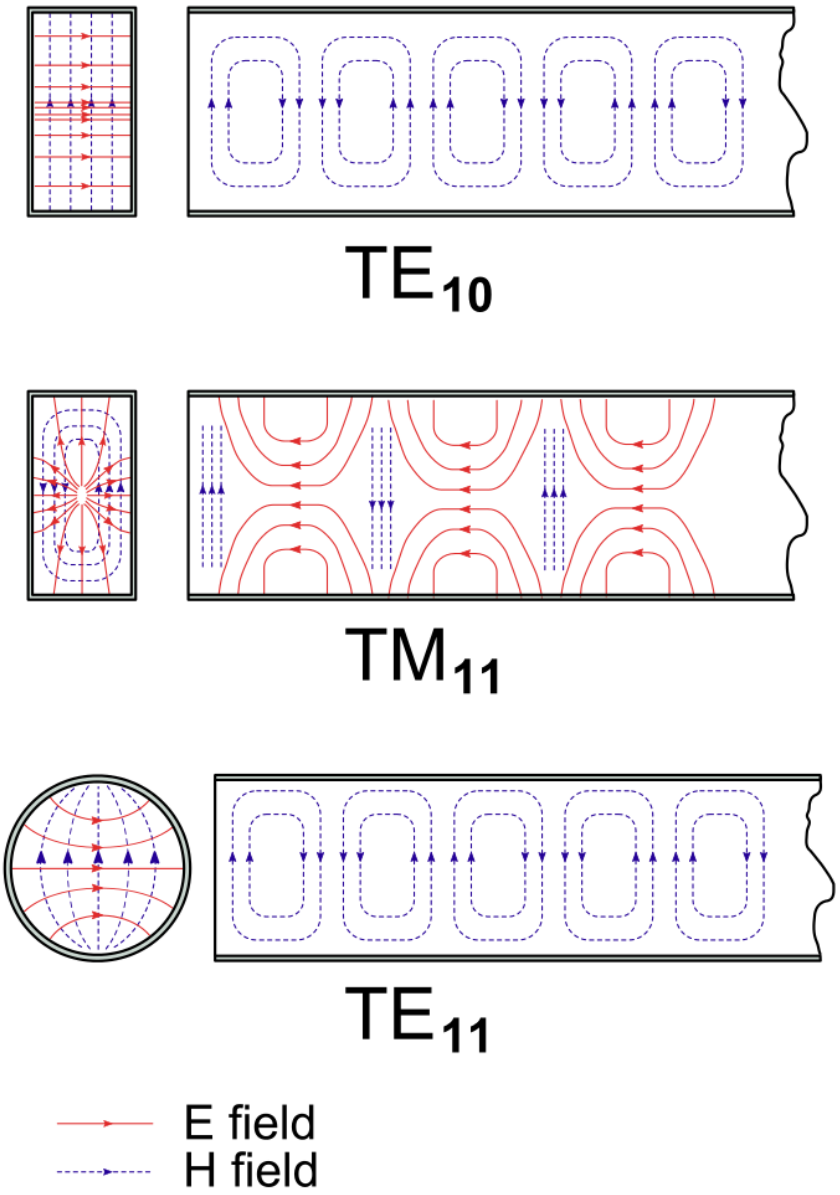

Figure 2.7: TE and TM modes in a waveguide

Include diagram from my own simulations

2.1.6 Confinement factor

Often it is necessary to know the confined power inside the core of the waveguide which helps in figuring out the waveguide mode. The confinement is also a measure of the

proportion of the power in a given mode that lies within the core [37].

$$\text{Confinement factor } = \frac{\int_{-H/2}^{H/2} E_x^2(y)\,dy}{\int_{-\infty}^{\infty} E_x^2(y)\,dy} \tag{2.16}$$

Confinement factor is an important measure which is function of various factors like polarization, RI difference between the core and cladding, mode number etc.

2.1.7 Jones calculus

Polarized light can be represented using Jones calculus. Polarized light is represented using *Jones vector* and linear optical elements are represented by *Jones matrices*. When light crosses an optical element the resulting polarization of the emerging light is found by taking the product of the Jones matrix of the optical element and the Jones vector of the incident light. *Jones calculus* is only applicable to light that is **already fully polarized** [38].

2.1.7.1 Jones vector

The Jones vector describes the polarization of light in free space or another homogeneous isotropic non-attenuating medium, where the light can be properly described as transverse waves [38]. The Jones vector is a complex vector that is a mathematical representation of a real wave. A typical representation of the electric field for the optical wave described in 2.8 can be as follows:

$$E = \begin{pmatrix} E_x(t) \\ E_y(t) \\ 0 \end{pmatrix} = \begin{pmatrix} E_x e^{i(kz-\omega t+\phi_x)} \\ E_y e^{i(kz-wt+\phi_y)} \\ 0 \end{pmatrix} = \begin{pmatrix} E_x e^{i\phi_x} \\ E_y e^{i\phi_y} \\ 0 \end{pmatrix} e^{i(kz-\omega t)} \tag{2.17}$$

where ϕ_x and ϕ_y indicate the phasor notation. The Jones vector of the plane wave is described by:

$$\begin{pmatrix} E_x e^{i\phi_x} \\ E_y e^{i\phi_y} \end{pmatrix} \tag{2.18}$$

and the intensity of the optical, I wave can be written as,

$$I = |E_x|^2 + |E_y|^2 \tag{2.19}$$

Generally, when considering Jones vector a wave of unit intensity is required for the consideration polarization, so Jones vector is noted using an unit vector where,

$$E\overline{E} = 1 \tag{2.20}$$

where $\overline{E}$ is the complex conjugate of E. In general the Jones representation of a normalized elliptically polarized beam with azimuth θ and elliptical angle ϵ is given by,

$$e^{i\phi} \begin{pmatrix} \cos\theta\cos\epsilon - j\sin\theta\sin\epsilon \\ \sin\theta\cos\epsilon - j\cos\theta\sin\epsilon \end{pmatrix} \tag{2.21}$$

where $e^{i\phi}$ is an arbitrary phase vector and $\phi = \phi_x - \phi_y$. So, for example a linear polarization of TE mode can be represented as,

$$\begin{pmatrix} 1 \\ 0 \end{pmatrix} \tag{2.22}$$

since, $\theta = 0$ and $\epsilon = 0$.

2.1.7.2 Jones matrix

Jones matrix are the formal representation of the various optical elements such as lenses, beam splitters, mirrors, phase retarders, polarizers at arbitrary angles that can modify polarization. They generally operate on Jones vector and helps in comprehend situations which light encounters multiple polarization elements in sequence. In these situations the products of the Jones matrices can be used to represent the transfer matrix. This situation can be represented using,

$$[E_{output}] = J_{system}[E_{input}] \tag{2.23}$$

where E_input is the input field into the optical system and E_output is the generated output field represented using Jones vector. The matrix J_system is the Jones matrix of the optical system comprising of a series of polarization devices. If there are N devices in the system then the final transfer matrix comes out as,

$$J_{system} = J_N J_{N-1} \ldots\ldots J_2 J_1 \tag{2.24}$$

where J_N is the Jones matrix for n^{th} polarizing optical element.

2.1.8 Jones matrix for polarizing optical systems

To construct optical waveguides for polarization rotation it is imperative to deal with the basic principles of standard available optical systems. Here, the fundamental principles of polarizer and wave plates are interpreted using Jones calculus.

2.1.8.1 Polarizer

Polarizers have an index of refraction which depends on orientation electric field propagation. If any optical system has a transmission axis and an absorption axis for electric fields, then lights will be passed along he transmission axis and absorbed along the other axis. So, the Jones matrix of a polarizer making an angle θ with the X-axis will come out as,

$$\begin{pmatrix} \cos^2\theta & \sin\theta\cos\theta \\ \sin\theta\cos\theta & \sin^2\theta \end{pmatrix} \tag{2.25}$$

2.1.8.2 Wave plates

Wave plates are phase retarders which are made of birefringent crystals. Wave plates can be conceptualized as two polarizers kept apart at certain distance d, such that their polarization axes are apart orthogonally (90^0). The phase difference as light passes through this setup of thickness d is,

$$(k_{slow} - k_{fast})\, d = \frac{2\pi d}{\lambda_{vac}} \left(n_{slow} - n_{fast}\right) \tag{2.26}$$

In, general the Jones matrix for a wave plate is given by,

$$\begin{pmatrix} \cos^2\theta + \xi \sin^2\theta & \sin\theta\cos\theta - \xi\sin\theta\cos\theta \\ \sin\theta\cos\theta - \xi\sin\theta\cos\theta & \sin^2\theta + \xi\cos^2\theta \end{pmatrix} \tag{2.27}$$

where ξ is calculated based on the type of wave plate. The following equations addresses some general scenarios:

$$\begin{cases} \xi = e^{i\pi/2}, & \text{where}, (k_{slow} - k_{fast})\, d = \pi/2 + 2\pi m, \text{for quarter-wave plate} \\ \xi = e^{i\pi}, & \text{where}, (k_{slow} - k_{fast})\, d = \pi + 2\pi m, \text{for half-wave plate} \end{cases} \tag{2.28}$$

Similar concept is used in the construction of PR waveguides which will be discussed in later sections shortly.

2.1.9 Poincaré sphere and state of polarization

To view a complete representation of all the polarization ellipses generated using Jones vectors, a spherical structure with unit radius is used, which is known as Poincaré sphere. If the orientation in space of of the ellipse of polarization is determined by the azimuth, θ and ellipticity, ϵ then that point can be completely characterized by its longitude 2θ and latitude 2ϵ. The north and south poles represent the right-handed and left-handed circular polarization respectively. In general the diametrically opposite points represent pairs of orthogonal polarization. The SOP and its corresponding location in the Poincaré sphere is visualized in the Fig. 2.8. To go from one SOP to another the polarized light can be passed through various optical components which can be computed using the Jones matrix and the corresponding SOP can be depicted on the Poincaré sphere as well.

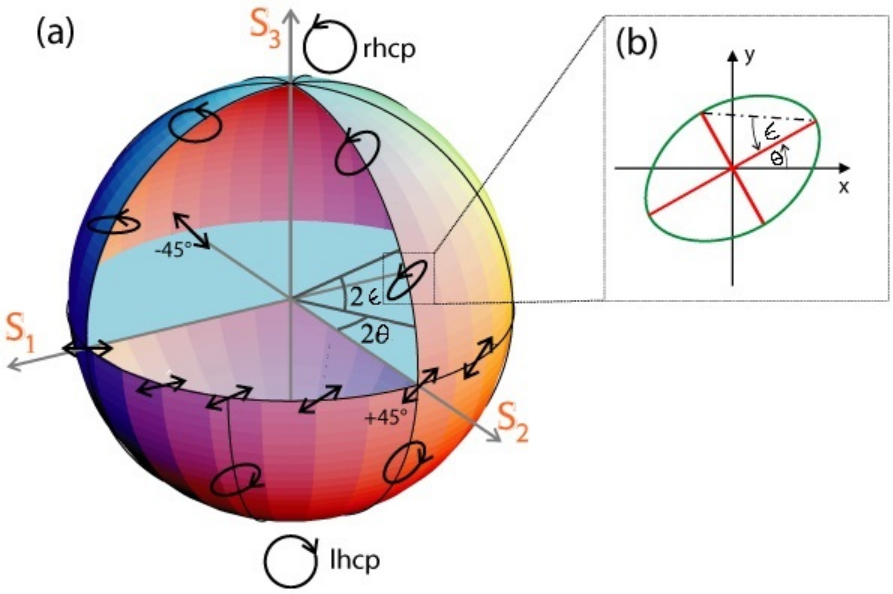

Figure 2.8: (a) Representation of the Poincaré sphere (b) Representation of the ellipse parameters [39]

The SOP of any wave is also defined using polarization extinction range/ratio (PER) and polarization phase, ϕ given by the following equations:

$$\begin{aligned} PER_{TE-TM} &= 10 \log \frac{P_{TM}}{P_{TE}} \\ PER_{TM-TE} &= 10 \log \frac{P_{TE}}{P_{TM}} \\ \phi &= \phi_x - \phi_y \end{aligned} \tag{2.29}$$

For complete polarized light, the point on the Poincaré sphere must be fixed on time which requires,

$$\frac{E_x\,(t)}{E_y\,(t)} = constant \tag{2.30}$$

and,

$$\phi = \phi_x(t) - \phi_y(t) = constant \tag{2.31}$$

2.1.10 Stoke's parameter

Quasi-monochromatic waves are mathematically treated using Stokes parameters (S_0, S_1, S_2, S_3), which constitute a vector generally known as Stokes vectors. Stokes vectors are used to keep track of the partial polarization (and attenuation) of a light beam in terms of total intensity (I), degree of polarization (p) and ellipse parameters, as the light progresses

through an optical system. A Stokes vector can generally be represented as,

$$\overrightarrow{S} = \begin{pmatrix} S_0 \\ S_1 \\ S_2 \\ S_3 \end{pmatrix} \tag{2.32}$$

where,

$$\begin{cases} S_0 = I \\ S_1 = I_p \cos 2\theta \cos 2\epsilon \\ S_2 = I_p \sin 2\theta \cos 2\epsilon \\ S_3 = I_p \sin 2\epsilon \end{cases} \tag{2.33}$$

Here, $I_p, 2\theta, 2\epsilon$ are the spherical coordinates of the 3-D vector of Cartesian coordinates (S_1, S_2, S_3). So, given the Stokes parameters, the spherical coordinates $(p, 2\theta, 2\epsilon)$ can be obtained and represented by a point inside the Poincaré sphere using the following:

$$\begin{cases} I = S_0 \\ p = \dfrac{\sqrt{S_1^2 + S_2^2 + S_3^2}}{S_0} \\ 2\theta = \tan^{-1} \dfrac{S_2}{S_1} \\ 2\epsilon = \tan^{-1} \dfrac{S_3}{\sqrt{S_1^2 + S_2^2}} \end{cases} \tag{2.34}$$

The prescribed notations are portrayed on the Poincaré sphere in the following Fig. 2.9.

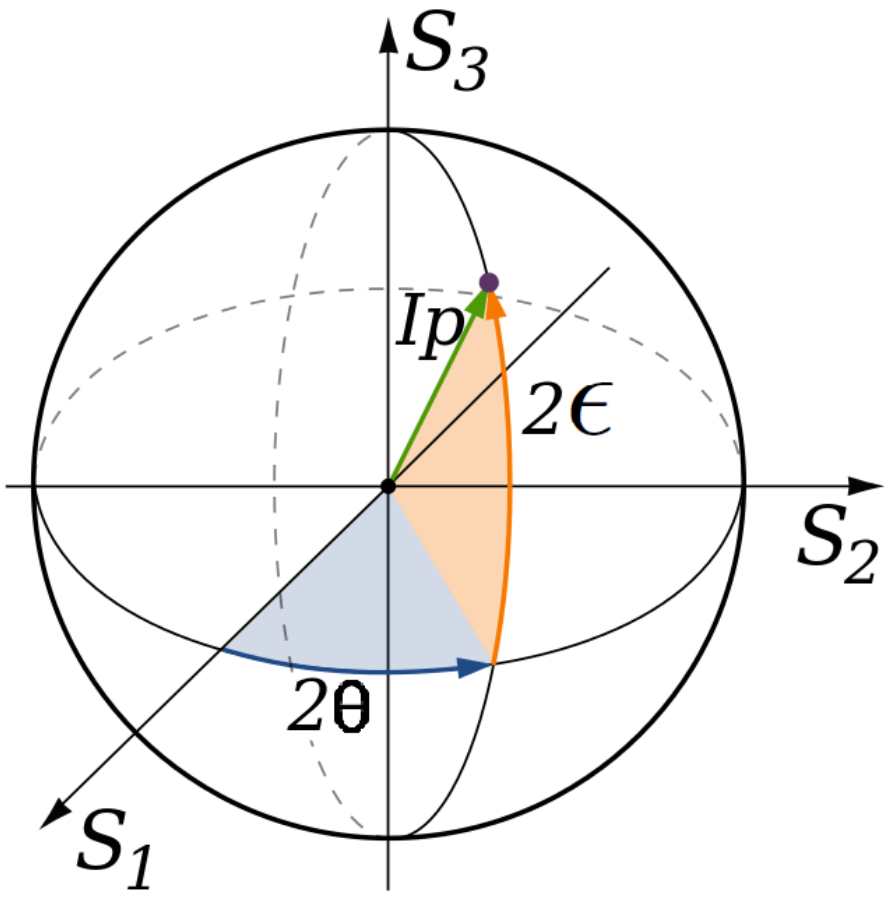

Figure 2.9: Poincaré sphere, on or beneath which the three Stokes parameters [S1, S2, S3] are plotted in Cartesian coordinates [40]

2.2 Tuning optical waveguide

2.2.1 Thermal mechanism

2.2.2 Liquid crystals

2.2.3 Current injection

2.2.4 MEMS

Actuation principle...

Why is MEMS better?

2.3 Polarization rotator (PR)

2.3.1 Optical fiber PR

2.3.2 Integrated circuit PR

The currently available PRs can be classified under two categories as passive and active PR. In the passive PRs the waveguide structures are designed in a specific way to manipulate the effective RI of the waveguide to obtain the desired polarization. The RI cannot be manipulated or tuned once fabricated. Whereas, in active PRs, the effective RI is manipulated by applying voltage to a fixed waveguide structure and using quantum optical phenomenon.

Revise

2.3.2.1 Passive PR

The passive PRs are based on the principles of mode evolution [41, 30, 42, 43, 44], mode coupling [28, 45, 27] and mode hybridization [46, 26, 47, 25] which are described in the following sections.

Mode evolution

Mode coupling

Mode hybridization

2.3.2.2 Active PR

2.3.2.3 Comparative analysis of available PR

Chapter 3

3 Design and simulation

3.1 Approach

3.2 Designing the experiment

3.2.1 Design principle

3.2.2 Use case: Active polarization rotator

3.3 Choice of simulation

3.4 Simulation results and analysis

Chapter 4

4 Fabrication

Chapter 5

5 Interpreting the design

5.1 Experimental setup for measurement

5.2 Optical coupling

5.3 Results

5.4 Analysis

Chapter 6

6 Conclusions

Chapter 7

7 Limitations and future work

7.1 Limitations

7.2 Future work

Todo list

Abbreviations

BPM Beam propagation method. 10

CAGR Compound annual growth rate. 4

CMOS Complementary metal-oxide semiconductor. 3, 4

EM Electromagnetic. 2, 6–8, 12

FDTD Finite difference time domain. 10

FEM Finite element modeling. 10

IC Integrated circuit(s). 3, 4

ICT Information and communication technology. 1

IMS IP Multimedia Subsystem. 2

IoT Internet of Things. 1

MEMS Microelectromechanical systems. 4, 5

OEIC Optoelectronic integrated circuit. 3, 4

PDλ Polarization dependent wavelength characteristics. 4

PDL Polarization dependent loss. 4

PER polarization extinction range/ratio. 17

PMD Polarization mode dispersion. 4

PR Polarization rotator. 4–6, 16, 20

RI Refractive index. 4, 8, 9, 11, 14, 20

SMC Single-mode condition. 10

SOI Silicon on Insulator. 4

SOP State of polarization. 6, 16, 17

TE Tansverse Electric. 9, 10, 12–15

TEM Tansverse Electromagnetic. 8, 12

TM Tansverse Magnetic. 9, 10, 12–14

TPR Tunable polarization rotator. 4, 5

Bibliography

[1] "Gartner says the internet of things installed base will grow to 26 billion units by 2020." http://www.gartner.com/newsroom/id/2636073, 2013. [Online; accessed 26-Jan-2016].

[2] "Number of Internet Users (2015) - Internet Live Stats." http://www.internetlivestats.com/internet-users/, 2015. [Online; accessed 22-Jan-2016].

[3] "What Happens in an Internet Minute [Infographic] | Daily Infographic." http://www.dailyinfographic.com/what-happens-in-an-internet-minute-infographic, 2013. [Online; accessed 29-Jan-2016].

[4] "Ericsson Mobility Report: 70 percent of world's population using smartphones by 2020." http://www.ericsson.com/news/1925907, 2015. [Online; accessed 06-Feb-2016].

[5] "Ericsson traffic exploration infograph." http://www.ericsson.com/TET/trafficView/loadBasicEditor.ericsson, 2015. [Online; accessed 06-Feb-2016].

[6] "ARK | Your Source for Intel® Product Specifications." http://ark.intel.com/, 2015. [Online; accessed 06-Feb-2016].

[7] "Silicon photonics." https://en.wikipedia.org/wiki/Silicon_photonics/, 2015. [Online; accessed 06-Feb-2016].

[8] N. Savage, "Linking Chips With Light." http://spectrum.ieee.org/semiconductors/optoelectronics/linking-chips-with-light, 2015. [Online; accessed 06-Feb-2016].

[9] E. Temprana, E. Myslivets, B. P.-P. Kuo, L. Liu, V. Ataie, N. Alic, and S. Radic, "Overcoming Kerr-induced capacity limit in optical fiber transmission," *Science*, vol. 348, pp. 1445–1448, June 2015.

[10] "Silicon photonics market to grow at CAGR of 38% from $25m in 2013 to $700m in 2024." http://www.semiconductor-today.com/news_items/2014/JUL/YOLE_180714.shtml, 2014. [Online; accessed 06-Feb-2016].

[11] B. Jalali and S. Fathpour, "Silicon Photonics," *Journal of Lightwave Technology*, vol. 24, pp. 4600–4615, Dec. 2006.

[12] M. C. Wu, T. J. Seok, S. Han, and N. Quack, "MEMS-Enabled Scalable Silicon Photonic Switches," *Optics Letters*, p. FW3B.2, 2015.

[13] D. Nikolova, S. Rumley, D. Calhoun, Q. Li, R. Hendry, P. Samadi, and K. Bergman, "Scaling silicon photonic switch fabrics for data center interconnection networks," *Optics Express*, vol. 23, p. 1159, Jan. 2015.

[14] L. Lu, L. Zhou, X. Li, and J. Chen, "Low-power 2x2 silicon electro-optic switches based on double-ring assisted Mach–Zehnder interferometers," *Optics Letters*, vol. 39, p. 1633, Mar. 2014.

[15] P. Dong, C. Xie, L. L. Buhl, Y.-K. Chen, J. H. Sinsky, and G. Raybon, "Silicon In-Phase/Quadrature Modulator With On-Chip Optical Equalizer," *Journal of Lightwave Technology*, vol. 33, pp. 1191–1196, Mar. 2015.

[16] C. Chen, C. He, D. Zhu, R. Guo, F. Zhang, and S. Pan, "Generation of a flat optical frequency comb based on a cascaded polarization modulator and phase modulator," *Optics Letters*, vol. 38, p. 3137, Aug. 2013.

[17] Y. Urino, Y. Noguchi, M. Noguchi, M. Imai, M. Yamagishi, S. Saitou, N. Hirayama, M. Takahashi, H. Takahashi, E. Saito, T. Shimizu, M. Okano, N. Hatori, M. Ishizaka, T. Yamamoto, T. Baba, T. Akagawa, S. Akiyama, T. Usuki, D. Okamoto, M. Miura, J. Fujikata, D. Shimura, H. Okayama, H. Yaegashi, T. Tsuchizawa, K. Yamada, M. Mori, T. Horikawa, T. Nakamura, and Y. Arakawa, "Demonstration of 12.5-Gbps Optical Interconnects Integrated with Lasers, Optical Splitters, Optical Modulators and Photodetectors on a Single Silicon Substrate," *Optics Letters*, p. Tu.4.E.1, 2012.

[18] C.-M. Chang, J. H. Sinsky, P. Dong, G. de Valicourt, and Y.-K. Chen, "High-power dual-fed traveling wave photodetector circuits in silicon photonics," *Optics Express*, vol. 23, p. 22857, Aug. 2015.

[19] S. Garcia and I. Gasulla, "Design of heterogeneous multicore fibers as sampled true-time delay lines," *Optics Letters*, vol. 40, p. 621, Feb. 2015.

[20] M. Mattarei, A. Canciamilla, S. Grillanda, and F. Morichetti, "Variable Symbol-Rate DPSK Receiver Based on Silicon Photonics Coupled-Resonator Delay Line," *Journal of Lightwave Technology*, vol. 32, pp. 3317–3323, Oct. 2014.

[21] S. Janz, A. Densmore, D.-x. Xu, P. Waldron, J. Lapointe, G. Lopinski, T. Mischki, P. Cheben, A. Delâge, B. Lamontagne, and J. H. Schmid, "Silicon Waveguide Photonics for Biosensing Applications," *Optics Letters*, p. IWA1, 2007.

[22] G. Lim, U. P. DeSilva, N. R. Quick, and A. Kar, "Laser optical gas sensor by photoexcitation effect on refractive index," *Applied Optics*, vol. 49, p. 1563, Mar. 2010.

[23] E. Ryckeboer, R. Bockstaele, M. Vanslembrouck, and R. Baets, "Glucose sensing by waveguide-based absorption spectroscopy on a silicon chip," *Biomedical Optics Express*, vol. 5, p. 1636, May 2014.

[24] A. Xie, L. Zhou, J. Chen, and X. Li, "Efficient silicon polarization rotator based on mode-hybridization in a double-stair waveguide," *Optics Express*, vol. 23, p. 3960, Feb. 2015.

[25] A. V. Velasco, M. L. Calvo, P. Cheben, A. Ortega-Moñux, J. H. Schmid, C. A. Ramos, i. M. Fernandez, J. Lapointe, M. Vachon, S. Janz, and D.-X. Xu, "Ultracompact polarization converter with a dual subwavelength trench built in a silicon-on-insulator waveguide," *Optics Letters*, vol. 37, p. 365, Feb. 2012.

[26] D. Leung, B. Rahman, and K. Grattan, "Numerical Analysis of Asymmetric Silicon Nanowire Waveguide as Compact Polarization Rotator," *IEEE Photonics Journal*, vol. 3, pp. 381–389, June 2011.

[27] J. Wang, B. Niu, Z. Sheng, A. Wu, X. Wang, S. Zou, M. Qi, and F. Gan, "Design of a SiO_2 top-cladding and compact polarization splitter-rotator based on a rib directional coupler," *Optics Express*, vol. 22, p. 4137, Feb. 2014.

[28] D. Dai and J. E. Bowers, "Novel concept for ultracompact polarization splitter-rotator based on silicon nanowires," *Optics Express*, vol. 19, p. 10940, May 2011.

[29] J. C. Wirth, J. Wang, B. Niu, Y. Xuan, L. Fan, L. Varghese, D. E. Leaird, and A. Weiner, "Efficient Silicon-on-Insulator Polarization Rotator based on Mode Evolution," *Optics Letters*, p. JW4A.83, 2012.

[30] L. Chen, C. R. Doerr, and Y.-K. Chen, "Compact polarization rotator on silicon for polarization-diversified circuits," *Optics Letters*, vol. 36, p. 469, Feb. 2011.

[31] J. D. Sarmiento-Merenguel, R. Halir, X. Le Roux, C. Alonso-Ramos, L. Vivien, P. Cheben, E. Durán-Valdeiglesias, I. Molina-Fernández, D. Marris-Morini, D.-X. Xu, J. H. Schmid, S. Janz, and A. Ortega-Moñux, "Demonstration of integrated polarization control with a 40 dB range in extinction ratio," *Optica*, vol. 2, p. 1019, Dec. 2015.

[32] M. Ibrahim, J. H. Schmid, A. Aleali, P. Cheben, J. Lapointe, S. Janz, P. J. Bock, A. Densmore, B. Lamontagne, R. Ma, D.-X. Xu, and W. N. Ye, "Athermal silicon waveguides with bridged subwavelength gratings for TE and TM polarizations," *Optics Express*, vol. 20, p. 18356, July 2012.

[33] Q. Xu, L. Chen, M. G. Wood, P. Sun, and R. M. Reano, "Electrically tunable optical polarization rotation on a silicon chip using Berry's phase," *Nature Communications*, vol. 5, p. 5337, Nov. 2014.

[34] G. Reed and A. Knights, *Silicon Photonics: An Introduction*. Wiley, 2004.

[35] "Wave–particle duality." `https://en.wikipedia.org/wiki/Wave%E2%80%93particle_duality`, Jan. 2016. [Online; accessed 07-Feb-2016].

[36] "Maxwell's equations." https://en.wikipedia.org/w/index.php?title=Maxwell%27s_equations&oldid=702587090, Jan. 2016. [Online; accessed 07-Feb-2016].

[37] G. T. Reed, *Silicon Photonics: The State of the Art*. New York, NY, USA: Wiley-Interscience, 2008.

[38] J. M. Burch and A. Gerald, *Introduction to Matrix Methods in Optics*. John Wiley & Sons, 1st ed., 1975.

[39] F. Flossmann, U. T. Schwarz, M. Maier, and M. R. Dennis, "Stokes parameters in the unfolding of an optical vortex through a birefringent crystal," *Optics Express*, vol. 14, no. 23, p. 11402, 2006.

[40] "Optical polarization waves." http://www.wikiwand.com/en/Polarization_(waves), 2015. [Online; accessed 09-Feb-2016].

[41] J. Zhang, M. Yu, G.-Q. Lo, and D.-L. Kwong, "Silicon-waveguide-based mode evolution polarization rotator," *Selected Topics in Quantum Electronics, IEEE Journal of*, vol. 16, pp. 53–60, Jan 2010.

[42] H. "Zhang, S. Das, J. Zhang, Y. Huang, C. Li, S. Chen, H. Zhou, M. Yu, P. Guo-Qiang Lo, and J. T. L. Thong, "Efficient and broadband polarization rotator using horizontal slot waveguide for silicon photonics," *Applied Physics Letters*, vol. 101, no. 2, 2012.

[43] J. C. Wirth, J. Wang, B. Niu, Y. Xuan, L. Fan, L. Varghese, D. E. Leaird, and A. Weiner, "Efficient silicon-on-insulator polarization rotator based on mode evolution," *Conference on Lasers and Electro-Optics 2012*, p. JW4A.83, 2012.

[44] K. Goi, A. Oka, H. Kusaka, K. Ogawa, T.-Y. Liow, X. Tu, G.-Q. Lo, and D.-L. Kwong, "Low-loss partial rib polarization rotator consisting only of silicon core and silica cladding," *Opt. Lett.*, vol. 40, pp. 1410–1413, Apr 2015.

[45] Y. Ding, H. Ou, and C. Peucheret, "Wideband polarization splitter and rotator with large fabrication tolerance and simple fabrication process," *Opt. Lett.*, vol. 38, pp. 1227–1229, Apr 2013.

[46] H. Fukuda, K. Yamada, T. Tsuchizawa, T. Watanabe, H. Shinojima, and S. ichi Itabashi, "Polarization rotator based on silicon wire waveguides," *Opt. Express*, vol. 16, pp. 2628–2635, Feb 2008.

[47] D. Vermeulen, S. Selvaraja, P. Verheyen, P. Absil, W. Bogaerts, D. Van Thourhout, and G. Roelkens, "Silicon-on-insulator polarization rotator based on a symmetry breaking silicon overlay," *Photonics Technology Letters, IEEE*, vol. 24, pp. 482–484, March 2012.